

Article

Performance of a Composite Thermoelectric Generator with Different Arrangements of SiGe, BiTe and PbTe under Different Configurations

Alexander Vargas-Almeida ^{1,†}, Miguel Angel Olivares-Robles ^{2,†,*} and Federico Méndez Lavielle ¹

¹ Departamento de Termofluidos, Facultad de Ingeniería, Universidad Nacional Autónoma de México, Mexico 04510, Mexico; E-Mails: alexvargas.almeida@gmail.com (A.V.-A.); fmendez@unam.mx (F.M.L.)

² Instituto Politecnico Nacional, SEPI ESIME-CUL, Av. Santa Ana 1000, Culhuacan, Coyoacan 04430, Mexico

[†] These authors contributed equally to this work.

* Author to whom correspondence should be addressed; E-Mail: olivares67@mailaps.org; Tel.: +52-555-729-6000 (ext. 73262); Fax: +52-555-656-2058.

Academic Editor: Kevin H. Knuth

Received: 21 July 2015 / Accepted: 20 October 2015 / Published: 28 October 2015

Abstract: In this study, we analyze the role of the thermoelectric (TE) properties, namely Seebeck coefficient α , thermal conductivity κ and electrical resistivity ρ , of three different materials in a composite thermoelectric generator (CTEG) under different configurations. The CTEG is composed of three thermoelectric modules (TEMs): (1) two TEMs thermally and electrically connected in series (SC); (2) two branches of TEMs thermally and electrically connected in parallel (PSC); and (3) three TEMs thermally and electrically connected in parallel (TEP). In general, each of the TEMs have different thermoelectric parameters, namely a Seebeck coefficient α , a thermal conductance K and an electrical resistance R . Following the framework proposed recently, we show the effect of: (1) the configuration; and (2) the arrangements of TE materials on the corresponding equivalent figure of merit Z_{eq} and consequently on the maximum power P_{max} and efficiency η of the CTEG. Firstly, we consider that the whole system is formed of the same thermoelectric material ($\alpha_1, K_1, R_1 = \alpha_2, K_2, R_2 = \alpha_3, K_3, R_3$) and, secondly, that the whole system is constituted by only two different thermoelectric materials

($\alpha_i, K_i, R_i = \alpha_j, K_j, R_j \neq \alpha_l, K_l, R_l$, where i, j, l can be 1, 2 or 3). In this work, we propose arrangements of TEMs, which clearly have the advantage of a higher thermoelectric figure of merit value compared to a conventional thermoelectric module. A corollary about the Z_{eq-max} for CTEG is obtained as a result of these considerations. We suggest an optimum configuration.

Keywords: thermoelectric module; thermoelectric properties; figure of merit

1. Introduction

Converting heat into electricity is now considered as a way for the recovery of wasted energy in various processes [1,2], such as natural gas combustion, oil industry, automobile exhausts, heat treatment furnaces for metal and heat generated by domestic heaters and stoves. Thermoelectric technology represents a significant opportunity for harnessing the available thermal energy. Although thermoelectric devices have been applied since 1940 [3], for example in laser systems, aerospace vehicles, watches, small portable heaters and sensors [4,5], the goal is to get more efficient adaptive devices to new sizes covering many applications for everyday life, not only for industry.

This work has been motivated by the necessity to develop new perspectives for improving these devices. A way to develop new designs is to link them to thermodynamics and heat transfer.

A thermoelectric module (TEM) operates on the basis of the energy transport, entropy and charge carriers in a semiconductor material, which are involved in the Seebeck and Peltier effects [6]. These effects can be analyzed by the reciprocal relations of Onsager [7], which express a certain symmetry in the mutual interference of two or more irreversible processes occurring simultaneously in a system (electric conduction and heat conduction are the irreversible processes that appear when an electric field is applied to a TEM) [7].

The important parameters of the Onsager's approach are the kinetic coefficients $L_{i,j}$, that for the particular case of the thermoelectric effects are given by,

$$\begin{aligned} L_{11} &= \frac{T}{e^2} \frac{1}{\rho} \\ L_{12} &= -\frac{T^2}{e^2} \frac{1}{\rho} S \\ L_{22} &= \frac{T^3}{e^2} \frac{1}{\rho} S^2 + T^2 \kappa \end{aligned} \quad (1)$$

where S is the entropy per carrier, e is the electron charge, ρ is the electrical resistance, κ is the thermal conductivity and T is the temperature.

The heat and current flows can be written in terms of kinetic coefficients, which are related to thermoelectric properties, such as thermal and electrical conductivity [7]. From Equations (1), it is possible to define the thermoelectric coefficients,

$$\begin{aligned}
\text{Peltier coefficient } \Pi_{AB} &= \frac{T}{e}(S^B - S^A) \\
\text{Thomson coefficient } \tau &= \frac{T}{e} \frac{dS}{dT} \\
\text{Seebeck coefficient } \alpha_{AB} &= \frac{1}{e}(S^B - S^A)
\end{aligned} \tag{2}$$

One of the most relevant parameters of a thermoelectric system, which combines the coefficients (2) and gives a measure of the efficiency of the TEM, is the thermoelectric figure of merit Z [8],

$$Z = \frac{\alpha^2}{\rho\kappa} \tag{3}$$

The Seebeck coefficient α is the generated voltage per unit of temperature. This coefficient is a main property of the material, and it is related to the carrier charge transport. It should be noted that α is directly proportional to the entropy transported by the flux of carriers S , which is given by the following relationship,

$$S = e\alpha \tag{4}$$

Diverse strategies have been developed for improving the figure of merit through optimization of the materials and the thermoelectric devices [9–13]. One of them is the combination of segments of different materials to form the legs of a thermocouple, but with the condition that these materials satisfy the criterion of compatibility, proposed by Snyder [14,15]. This approach combines a thermodynamic analysis with the study of thermoelectric properties (α , ρ , κ). In this approach, the main quantity is the compatibility factor s ,

$$s = \frac{\sqrt{1 + ZT} - 1}{\alpha T} \tag{5}$$

where Z is the figure of merit, T is the average temperature and α is the Seebeck coefficient.

According to the information mentioned above, it is important to analyze the impact of the Seebeck coefficient on the system's performance to understand the behavior of a thermoelectric system under different configurations. On the physics of the Seebeck coefficient, we briefly mention that when a metal is submitted to a temperature difference, $\Delta T = T_h - T_c$, in the ends with ($T_h > T_c$), there exists a net diffusion of electrons from the hot end towards the cold end, due to the energetic difference between electrons in the hot end at T_h and the cold end at T_c . This fact leaves behind exposed positive metal ions in the hot region and accumulates electrons in the cold region. This situation prevails until the electric field development between the positive ions in the hot region and the excess electrons in the cold region prevents further electron motion from the hot to cold side [16]. A voltage ΔV is therefore developed between the hot and cold ends with the hot end at the positive potential. Both quantities ΔV and ΔT are related by the next equation,

$$\alpha = \frac{\Delta V}{\Delta T} \tag{6}$$

In this work, we consider a thermoelectric system composed of conventional and segmented TEMs connected in different ways. To achieve this goal, we use the new approach proposed by Goupil and Apertet [17,18], in which a thermoelectric module is considered as an equivalent thermal-electrical circuit (see Figure 1). Following these methods, we derive the figure of merit of these systems.

In the following sections, we show the obtained results by applying this new approach.

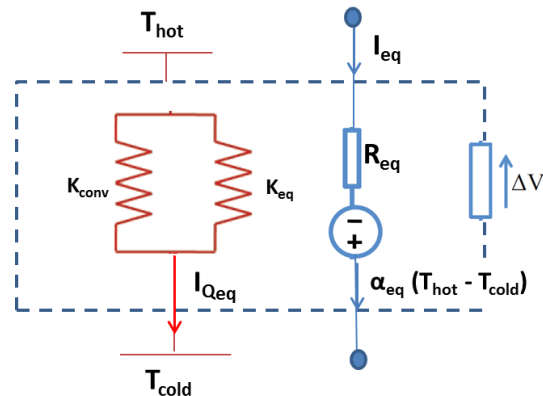


Figure 1. Thermoelectric generator and its representation as a thermal-electrical circuit.

2. Composite Thermoelectric Generator

2.1. Configuration of Thermal and Electrical Connections

In this work, we consider a thermoelectric system composed of three thermoelectric modules (TEMs) recently proposed by [19]. We study the three different configurations of a composite thermoelectric generator (CTEG), namely, (1) a two-stage CTEG thermally and electrically connected in series (SC); (2) a segmented-conventional CTEG thermally and electrically connected in parallel (PSC); and (3) three conventional TEMs connected thermally and electrically in parallel (TEP). These configurations are shown in Figures 2–4. We use the same assumptions and notation used above [19], *i.e.*, the internal electrical resistance, R , the thermal conductance under an open electrical circuit condition, K , and the Seebeck coefficient, α , which does not vary with the temperature.

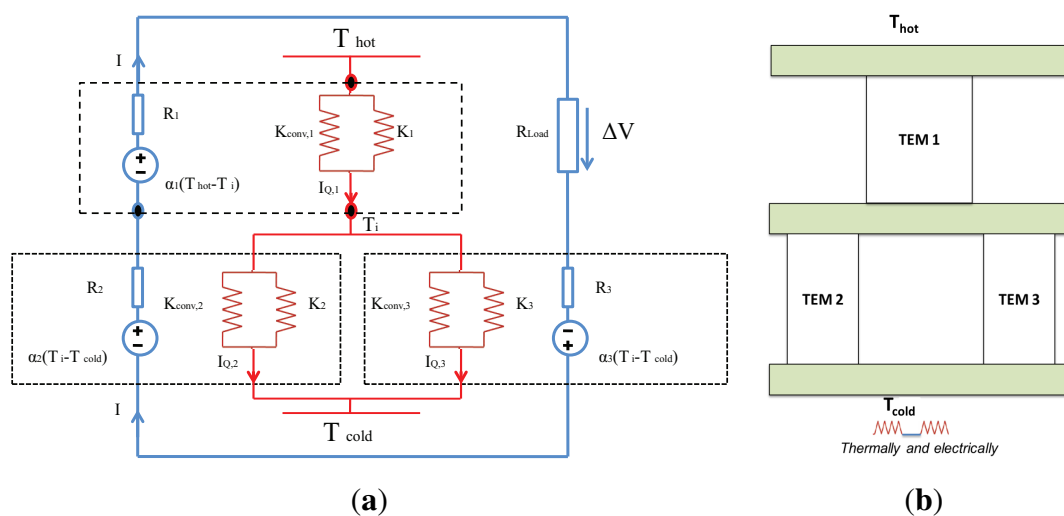


Figure 2. (a) Thermal-electrical circuit of series connected thermoelectric generator (SC-TEG), which is composed of two stages, which are thermally and electrically connected in series; (b) SC-composite TEG (CTEG) system.

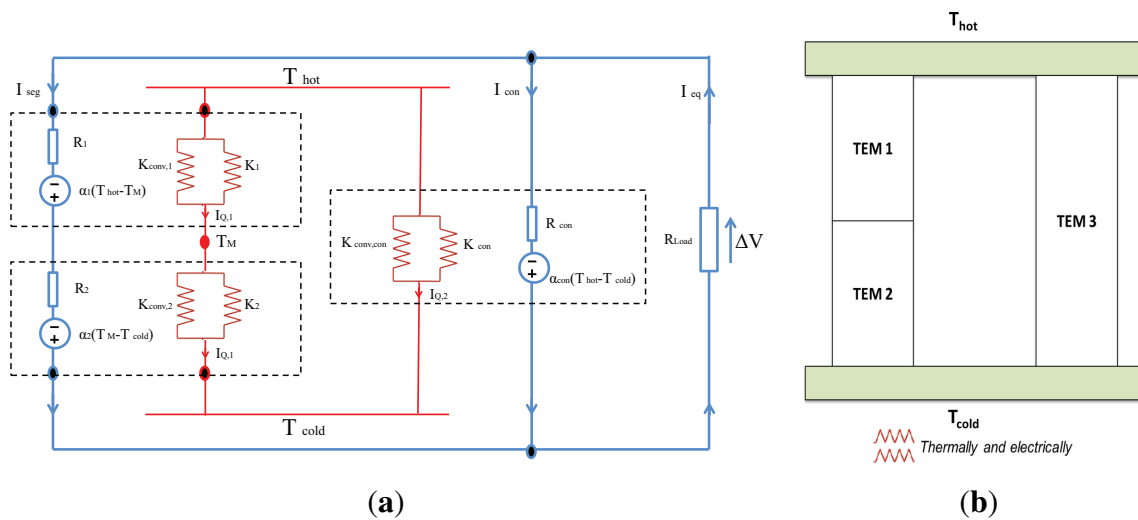


Figure 3. (a) Thermal-electrical circuit of a parallel series connected (PSC)-CTEG composed of segmented-conventional TEMs, which are thermally and electrically connected in parallel; (b) PSC-CTEG composite system.

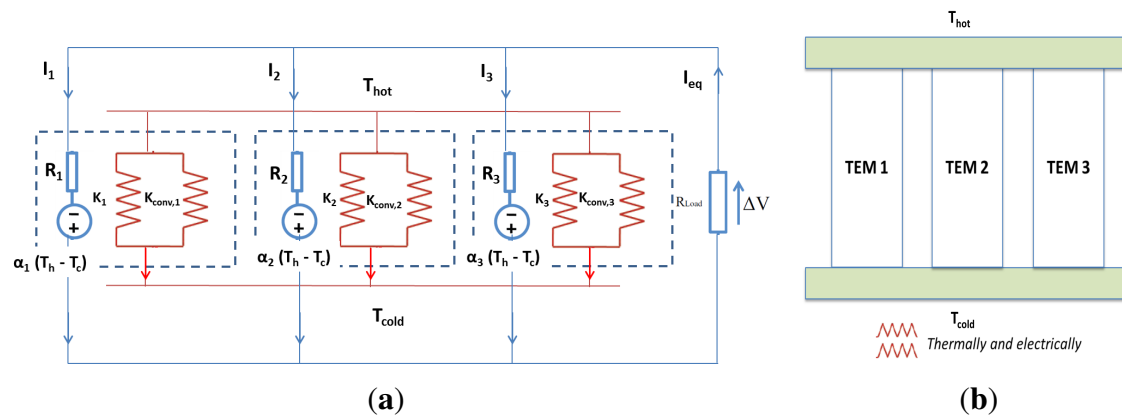


Figure 4. (a) Thermal-electrical circuit of thermally and electrically in parallel (TEP)-CTEG composed of three conventional TEMs, which are thermally and electrically connected in parallel; (b) TEP-CTEG composite system.

2.2. Equivalent Figure of Merit for Different Configurations

Following the framework recently proposed by Goupil *et al.* [18], the figures of merit can be easily derived for each of the systems mentioned above [19],

$$Z_{eq-SC} = \frac{\left[\frac{-(\alpha_2 + \alpha_3)K_1 - \alpha_1 K_2 - \alpha_1 K_3}{K_1 + K_2 + K_3} \right]^2}{\left[\frac{(\alpha_1 - \alpha_2 - \alpha_3)^2 T}{K_1 + K_2 + K_3} + (R_1 + R_2 + R_3) \right] \left[\frac{K_1(K_2 + K_3)}{K_1 + K_2 + K_3} \right]} \quad (7)$$

$$Z_{eq-PSC} = \frac{\left(\frac{\frac{\alpha_s}{R_s} + \frac{\alpha_c}{R_c}}{\frac{1}{R_s} + \frac{1}{R_c}} \right)^2}{\left[\frac{R_s R_c}{R_c + R_s} \right] \left[K_s + K_c + \frac{1}{\frac{1}{R_s} + \frac{1}{R_c}} (\alpha_s - \alpha_c)^2 T \right]} \quad (8)$$

$$Z_{eq-TEP} = \frac{\left(\frac{R_3 \left(\frac{\alpha_1 R_2 + \alpha_2 R_1}{R_1 + R_2} \right) + \left(\frac{R_1 R_2}{R_1 + R_2} \right) \alpha_3}{R_3 + \frac{R_1 R_2}{R_1 + R_2}} \right)^2}{\left(\frac{\frac{R_1 R_2 R_3}{R_1 + R_2}}{R_3 + \frac{R_1 R_2}{R_1 + R_2}} \right) \left(K_1 + K_2 + K_3 + \frac{(\alpha_1 - \alpha_2)^2 T}{R_1 + R_2} + \frac{\left(\frac{\alpha_1 R_2 - \alpha_2 R_1}{R_1 + R_2} - \alpha_3 \right)^2 T}{\frac{R_1 R_2}{R_1 + R_2} + R_3} \right)} \quad (9)$$

3. Arrangements for Thermoelectric Materials in TEGS

We study the role of the thermoelectric properties in the CTEG. Firstly, we consider the configuration effect, and secondly, we study the role of the thermoelectric properties in the composite CTEG.

3.1. Case I: Homogeneous Thermoelectric Properties, Configuration Effect

In this case, we consider each configuration of the TEMs with the same thermoelectric material, $(\alpha_1, K_1, R_1) = (\alpha_2, K_2, R_2) = (\alpha_3, K_3, R_3)$;

Homogeneous SC TEGS:

$$Z_{eq-SC}^h = \frac{\left(\frac{-4\alpha_i}{3} \right)^2}{\left(\frac{(-\alpha_i)^2 T}{3K_i} + 3R_i \right) \left(\frac{2K_i}{3} \right)} \quad (10)$$

Homogeneous PSC TEGS:

$$Z_{eq-PSC}^h = \frac{(\alpha_i)^2}{\left(\frac{2R_i}{3} \right) \left(\frac{3K_i}{2} \right)} \quad (11)$$

Homogeneous TEP TEGS:

$$Z_{eq-TEP}^h = \frac{(\alpha_i)^2}{\left(\frac{R_i}{3} \right) \left(3K_i + \frac{2(\alpha_i)^2 T}{3R_i} \right)} \quad (12)$$

where $i = (\text{BiTe}, \text{PbTe} \text{ or } \text{SiGe})$.

3.2. Case II: Heterogeneous Thermoelectric Properties, Arrangements of Thermoelectric Materials

For this case, we consider the three configurations described above, but with two equal materials and the other one different. Thus, two TEMs have the same semiconductor material and the other one a different semiconductor material.

Heterogeneous SC-TEGS:

$$Z_{eq-SC}^{Inh} = \frac{\left(\frac{-(\alpha_j + \alpha_l)K_i - \alpha_i(K_j + K_l)}{K_i + K_j + K_l} \right)^2}{\left(\frac{(\alpha_i - \alpha_j - \alpha_l)^2 T}{K_i + K_j + K_l} + R_i + R_j + R_l \right) \left(\frac{K_i(K_j + K_l)}{K_i + K_j + K_l} \right)} \quad (13)$$

Heterogeneous PSC-TEGS:

$$Z_{eq-PSC}^{Inh} = \frac{\left(\frac{R_l \left(\frac{K_j \alpha_i + K_i \alpha_j}{K_i + K_j} \right) + \left(R_i + R_j + \frac{(\alpha_i - \alpha_j)^2 T}{K_i + K_j} \right) \alpha_l}{R_i + R_j + R_l + \frac{(\alpha_i - \alpha_j)^2 T}{K_i + K_j}} \right)^2}{\left(\frac{R_l \left(R_i + R_j + \frac{(\alpha_i - \alpha_j)^2 T}{K_i + K_j} \right)}{R_l + R_i + R_j + \frac{(\alpha_i - \alpha_j)^2 T}{K_i + K_j}} \right) \left(\frac{K_j K_i}{K_i + K_j} + K_l + \left(\frac{K_j \alpha_i + K_i \alpha_j}{K_i + K_j} - \alpha_l \right)^2 \frac{T}{R_i + R_j + R_l + \frac{(\alpha_i - \alpha_j)^2 T}{K_i + K_j}} \right)} \quad (14)$$

Heterogeneous TEP-TEGS:

$$Z_{eq-EPT}^{Inh} = \frac{\left(\frac{R_l \left(\frac{\alpha_i R_j + \alpha_j R_i}{R_i + R_j} \right) + \left(\frac{R_i R_j}{R_i + R_j} \right) \alpha_l}{R_l + \frac{R_i R_j}{R_i + R_j}} \right)^2}{\left(\frac{\frac{R_i R_j R_l}{R_i + R_j}}{R_l + \frac{R_i R_j}{R_i + R_j}} \right) \left(K_i + K_j + K_l + \frac{(\alpha_i - \alpha_j)^2 T}{R_i + R_j} + \frac{\left(\frac{\alpha_i R_j - \alpha_j R_i}{R_i + R_j} - \alpha_l \right)^2 T}{\frac{R_i R_j}{R_i + R_j} + R_l} \right)} \quad (15)$$

4. Results and Discussion

Now, we show our results for the two cases mentioned above: the first is analyzed by applying Equations (10)–(12) matching the three modules to the same material; the second case is studied by applying Equations (13)–(15) using different arrangements of thermoelectric material when ($i = j \neq l$); ($i = l \neq j$); ($j = l \neq i$) where ($i; j; l$) can be any of the thermoelectric materials (BiTe, PbTe, SiGe).

4.1. Homogeneous TEGS: Effect of the Configuration

In this first case, we are interested in the effect of the configuration of the CTEG on the equivalent figure of merit, Z_{eq} . We consider the case when the three TEMs have the same thermoelectric material, *i.e.*, $(\alpha_1, K_1, R_1) = (\alpha_2, K_2, R_2) = (\alpha_3, K_3, R_3)$ or, equivalently, $TEM_1 = TEM_2 = TEM_3$. Table 1 shows our numerical values obtained for the equivalent figure of merit Z_{eq}^h of the considered configurations.

Table 1. Numerical values of Z_{eq}^h , for each of the three configurations using different materials.

Material	Z_{eq-SC}^h	Z_{eq-PSC}^h	Z_{eq-TEP}^h
BiTe	0.00212133	0.00305269	0.00195898
PbTe	0.00055109	0.000657238	0.000586714
SiGe	0.000287562	0.00033337	0.000314212

Notice that different values of the figure of merit Z_{eq}^h for each configuration are obtained when the three thermoelectric modules are made with the same thermoelectric material, *i.e.*, $TEM_1 = TEM_2 = TEM_3$. The highest value of Z_{eq}^h in each configuration is reached when we use BiTe; the most efficient configuration corresponds to when the TEMs are connected thermally and electrically in parallel $Z_{eq} > 0.0030$, while the least efficient configuration corresponds when we use SiGe as the thermoelectric material and the TEMs is connected electrically and thermally in series.

4.2. Heterogeneous TEGs: Different Arrangements of Thermoelectric Materials

In this section, we analyze the effect of thermoelectric materials arrangements on the equivalent figure of merit, Z_{eq} , for each configuration. For this case, we consider that $TEM_i = TEM_j$, i.e., two TEMs are made of the same thermoelectric material and the third TEM_l is made of a different thermoelectric material. Thus, we have three possibilities ($TEM_1 = TEM_2 \neq TEM_3$, $TEM_1 = TEM_3 \neq TEM_2$, $TEM_2 = TEM_3 \neq TEM_1$) for each configuration. Notice that each arrangement has six different combinations if the cyclical order of the material is taken into account. Thus, for each system, SC, PSC and TEP, we have eighteen possible combinations. Figures 5–7 show the behavior of Z_{eq} in terms of the intrinsic thermal conductances ratio $K_{i,j}/K_l$ for the optimal cases of each configuration, and Tables 2–4 show the maximum values of the figure of merit Z_{eq-max} , respectively.

From Tables 2–4, it must be noted that for each of the three configurations of the CTEG, there are most efficient material arrangements in each configuration when $TEM_i = TEM_j \neq TEM_l$. Table 5 shows each configuration with the most efficient material arrangements for each TEM.

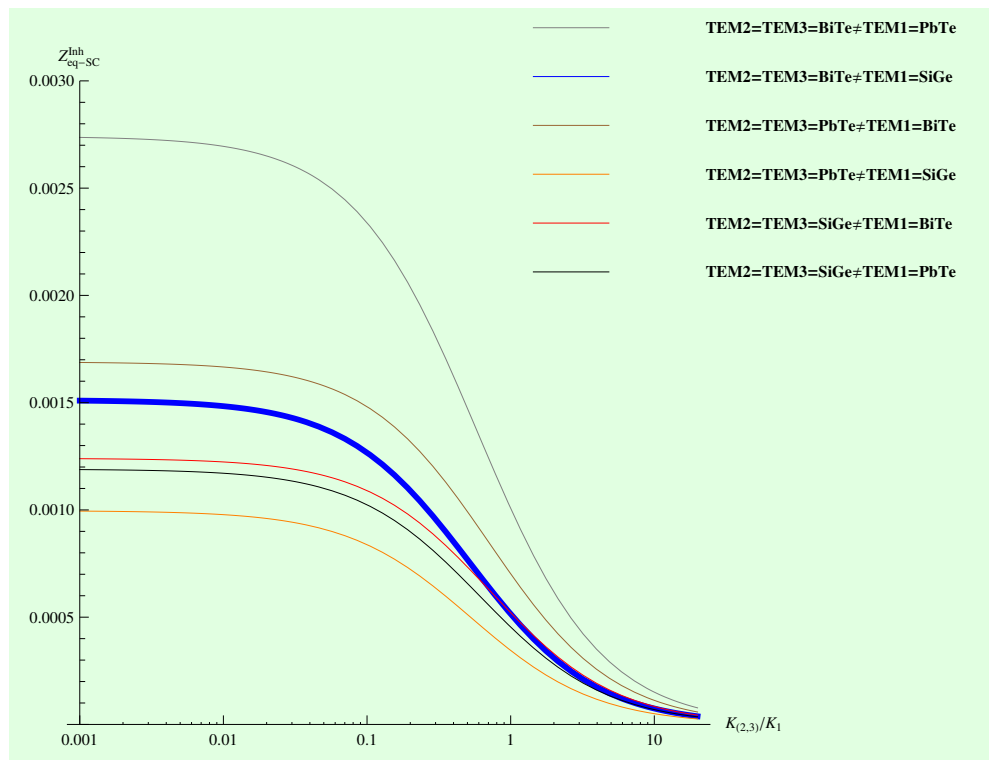


Figure 5. The equivalent figure of merit corresponding to heterogeneous SC CTEG, under the condition $TEM_2 = TEM_3 \neq TEM_1$. The highest numerical value corresponding to $TEM_2 = TEM_3 = BiTe \neq TEM_1 = PbTe$.

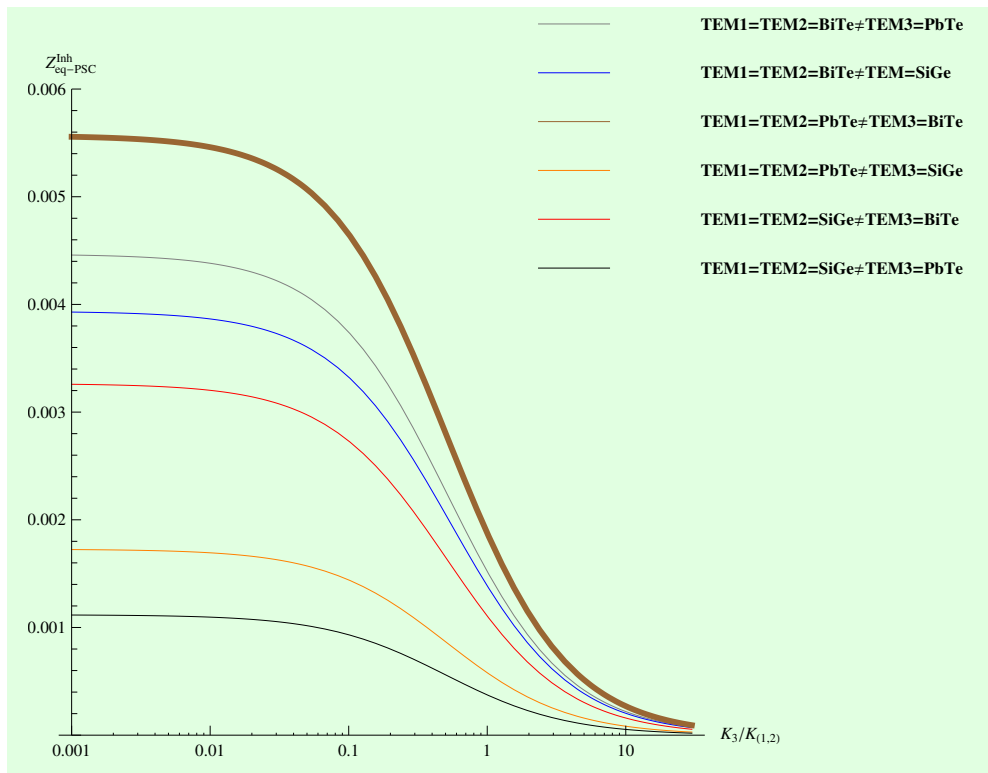


Figure 6. The equivalent figure of merit corresponding to heterogeneous PSC TEGS under the condition $TEM_1 = TEM_2 \neq TEM_3$. The highest numerical value corresponding to $TEM_1 = TEM_2 = PbTe \neq TEM_3 = BiTe$.

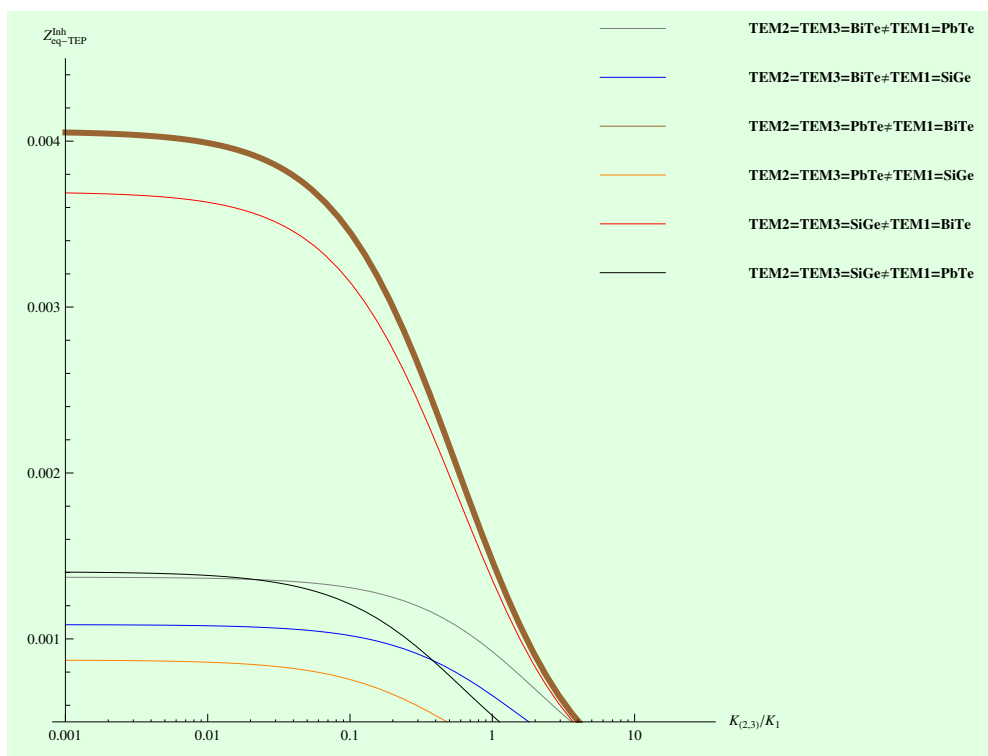


Figure 7. The equivalent figure of merit corresponding to the TEP TEGS under the condition $TEM_2 = TEM_3 \neq TEM_1$. The highest numerical value corresponding to $TEM_2 = TEM_3 = PbTe \neq TEM_1 = BiTe$.

Table 2. Numerical values of $Z_{eq-SC-max}^{Inh}$ for SC TEGS with the arrangement $TEM_i = TEM_j \neq TEM_l$.

TEM_1	$TEM_2 = TEM_3$	$Z_{eq-SC-max}^{Inh}$
BiTe	PbTe	0.00168734
	SiGe	0.0012388
PbTe	BiTe	0.00273649
	SiGe	0.00118802
SiGe	BiTe	0.00150947
	PbTe	0.000994534

Table 3. Numerical values of $Z_{eq-PSC-max}^{Inh}$ for PSC TEGS with the arrangement $TEM_i = TEM_j \neq TEM_l$.

TEM_3	$TEM_1 = TEM_2$	$Z_{eq-PSC-max}^{Inh}$
BiTe	PbTe	0.0055567
	SiGe	0.00325841
PbTe	BiTe	0.00445846
	SiGe	0.0011157
SiGe	BiTe	0.00392902
	PbTe	0.00172358

Table 4. Numerical values of $Z_{eq-TEP-max}^{Inh}$ from the TEP arrangement under condition $TEM_i = TEM_j \neq TEM - l$.

TEM_1	$TEM_2 = TEM_3$	$Z_{eq-TEP-max}^{Inh}$
BiTe	PbTe	0.00405227
	SiGe	0.00108556
PbTe	BiTe	0.00137141
	SiGe	0.000871679
SiGe	BiTe	0.00368808
	PbTe	0.00140252

Table 5. Most efficient arrangements in each case $TEM_i = TEM_j \neq TEM_l$.

System	Arrangement
SC	$TEM_2 = TEM_3 = BiTe \neq TEM_1 = PbTe$
PSC	$TEM_1 = TEM_2 = PbTe \neq TEM_3 = BiTe$
TEP	$TEM_2 = TEM_3 = PbTe \neq TEM_1 = BiTe$

Our results also show that the most efficient system of the three configurations is the PSC configuration with the corresponding material arrangement, namely $TEM_1 = TEM_2 = PbTe \neq TEM_3 = BiTe$; see Figure 8.

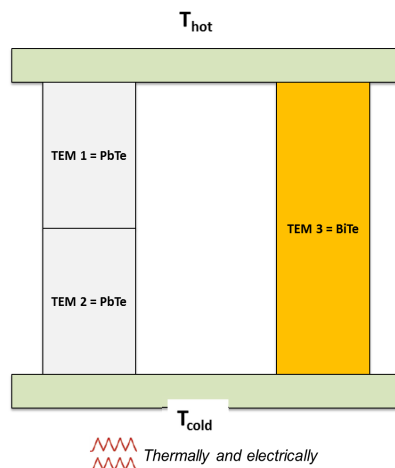


Figure 8. The optimal configuration corresponds to the PSC TEGS under the condition $TEM_1 = TEM_2 = PbTe \neq TEM_3 = BiTe$.

Furthermore, notice the effect of the position of the thermoelectric material in the CTEG through the TEMs on the equivalent thermoelectric figure of merit Z_{eq} of the system. It suggests that the CTEG works more efficiently depending on the position of a thermoelectric material in conjunction with other materials.

4.3. Maximum Power and Efficiency

The performance of a TEG is characterized by its thermal efficiency, such as a heat engine, and the generated electric power (from the point of view of energy conversion); both of them are functions of the figure of merit. In this section, we analyze the generated maximum power and the efficiency of the PSC system. We assumed that the maximum value of Z_{eq-PSC}^{Inh} can be reached.

4.3.1. Maximum Power

For the ideal model of a TEM, which does not take into account the effect of the heat sinks, the maximum electrical power delivered to the load is given by,

$$P_{max} = \frac{\alpha^2(T_H - T_C)^2}{4R} \quad (16)$$

However, when a TEM has coupled heat exchangers, it is necessary to consider a thermal contact conductance, K_c . We calculate the electrical power produced by the PSC system taking into account the thermal contact conductance and thermal conductance at zero electrical current. Thus, the maximum output power, using the corresponding maximum value of the equivalent figure of merit Z_{eq-PSC}^{Inh} , is given by [20],

$$P_{max-PSC} = \frac{(K_c \Delta T)^2}{4(K_{I=0} + K_c)\bar{T}} \frac{Z_{eq-PSC}^{Inh} \bar{T}}{1 + Z_{eq-PSC}^{Inh} \bar{T} + K_c/K_{I=0}} \quad (17)$$

Figure 9 shows maximum power values for the PSC system as a function of the ratio $K_{I=0}/K_c$, i.e., in terms of internal thermal conductance $K_{I=0}$ and the contact thermal conductance K_c , with the condition $TEM_1 = TEM_2 \neq TEM_3$.

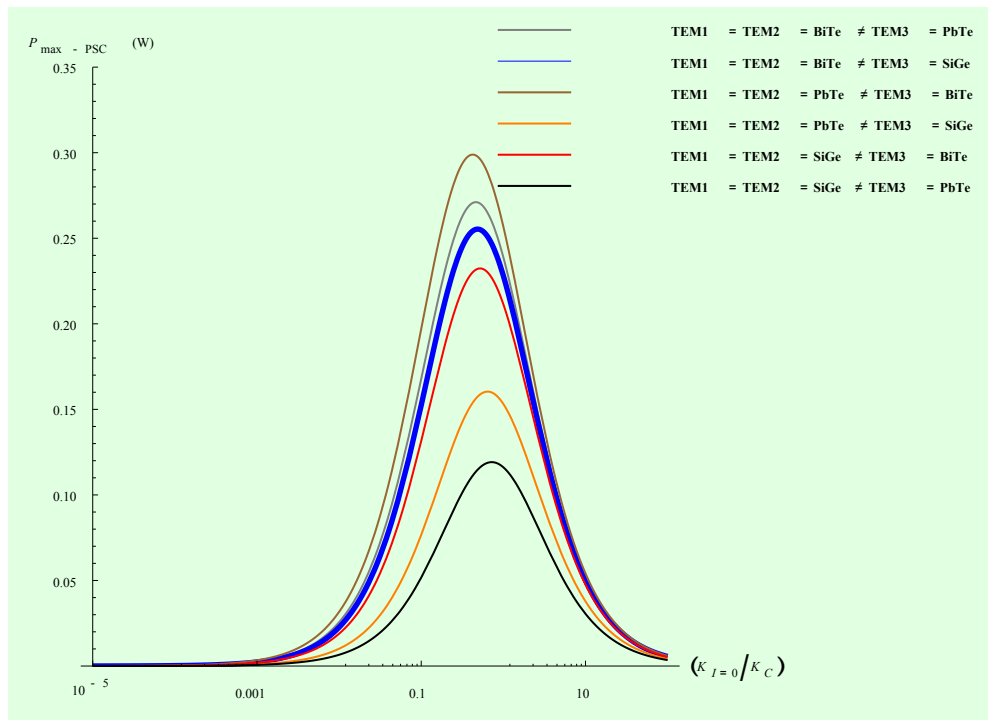


Figure 9. Maximum power of the system PSC under the condition $TEM_1 = TEM_2 \neq TEM_3$, the highest numerical value corresponding to case $TEM_1 = TEM_2 = PbTe \neq TEM_3 = BiTe$.

Figure 10 shows clearly the interval of values for the ratio $K_{I=0}/K_c$, where the maximum output power reaches its maximum values.

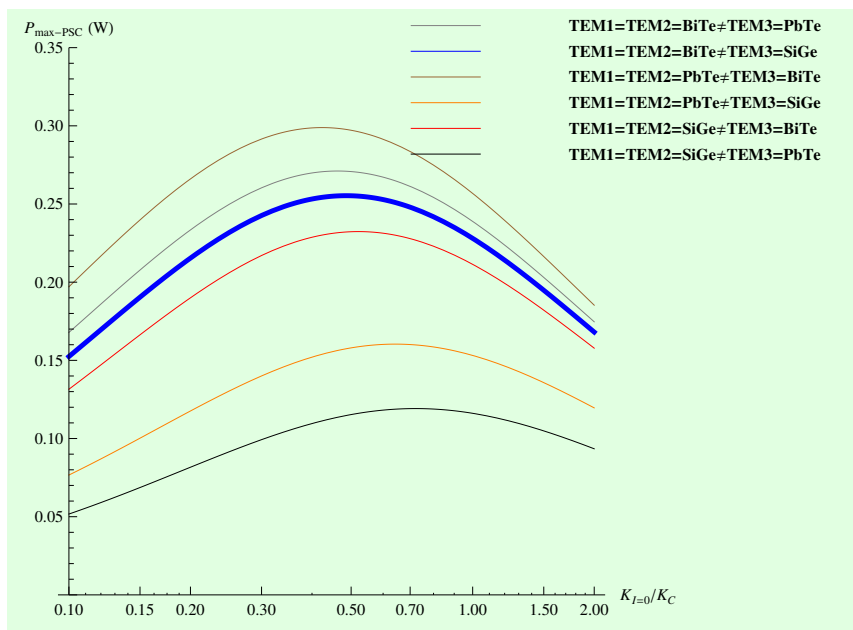


Figure 10. The output power of the system PSC reaches the maximum values.

We note from Figure 10 that each of the material arrangements has a characteristic value of $K_{I=0}/K_c$ in which the electrical power reaches maximum values. For example, when $TEM_1 = TEM_2 = PbTe \neq TEM_3 = BiTe$, the maximum value for the electrical power is between $K_{I=0}/K_c = 0.30$ and

$K_{I=0}/K_c = 0.50$. In fact, the PSC system reaches the maximum value of the electrical power at small values of the ratio $K_{I=0}/K_c$, compared to other systems, e.g., $TEM_1 = TEM_2 = SiGe \neq TEM_3 = PbTe$, which reaches maximum values between $K_{I=0}/K_c = 0.50$ and $K_{I=0}/K_c = 0.80$.

4.3.2. Efficiency

The efficiency of a thermoelectric generator as a function of Z is given by,

$$\eta = \frac{\Delta T}{T_H} \frac{\sqrt{1 + z\bar{T}} - 1}{\sqrt{1 + z\bar{T}} + \frac{T_C}{T_H}} \quad (18)$$

For the PSC system with the $TEM_1 = TEM_2 = PbTe \neq TEM_3 = BiTe$ arrangement, we replace Z by Z_{eq-PSC}^{Inh} ,

$$\eta_{eq-PSC}^{Inh} = \frac{\Delta T}{T_H} \frac{\sqrt{1 + Z_{eq-PSC}^{Inh}\bar{T}} - 1}{\sqrt{1 + Z_{eq-PSC}^{Inh}\bar{T}} + \frac{T_C}{T_H}} \quad (19)$$

Finally, for an ideal TEG, *i.e.*, without taking into account the heat exchangers, we can analyze the performance of the TEG considering (1) the intrinsic thermal conductances ratio ($K_3/K_{1,2}$) and (2) the electrical resistances ratio ($R_3/R_{1,2}$).

Figure 11 shows a contour plot for different values of η_{eq-PSC}^{Inh} as a function of the ratios, $K_3/K_{1,2}$ and $R_3/R_{1,2}$.

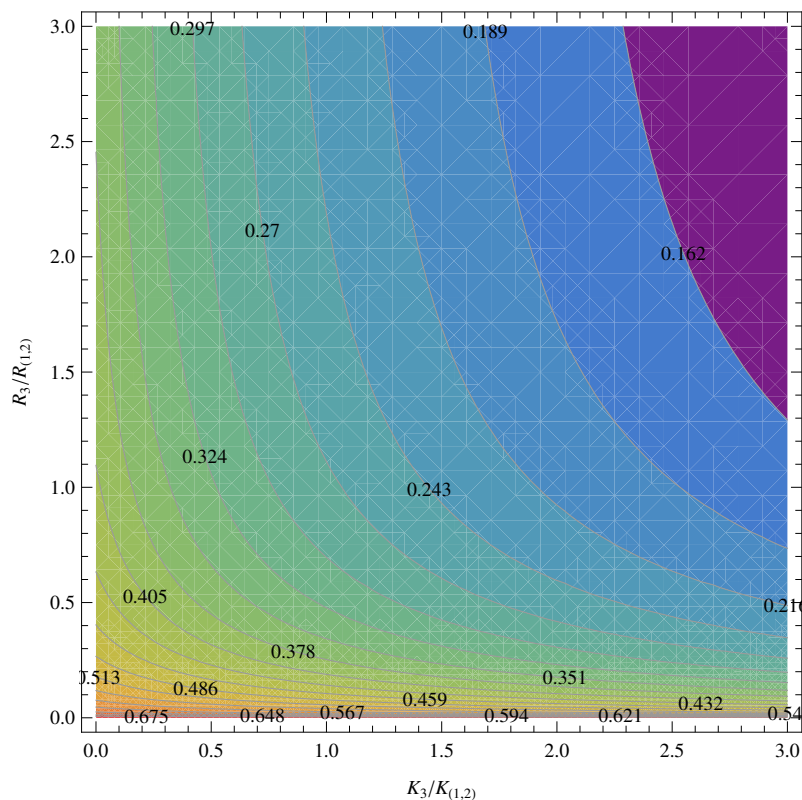


Figure 11. Contour plot: efficiency for the PSC-system assuming the condition $TEM_1 = TEM_2 \neq TEM_3$, assuming the maximum value of Z_{eq-PSC}^{Inh} ($TEM_1 = TEM_2 = PbTe \neq TEM_3 = BiTe$).

In Figure 11, we can observe that the range of optimal values for the best performance of a PSC composite TEG is between (0.1, 1.0) and (0.1, 0.5) for $K_3/K_{1,2}$ and $R_3/R_{1,2}$, respectively. It is remarkable that the thermal conductances ratio shows a wider range of good values in comparison with the electrical resistances ratio, which shows a more restricted range.

5. The Case of a Three-TEM Chain Thermally and Electrically Connected in Series

Finally, we consider a three-TEMs chain, which is a basic connection between thermoelectric elements that are thermally and electrically connected in series. This model corresponds to segmented branches in TEMs. Recently, an equivalent model of two thermoelectric generators in series has been studied [21]. However, the combination of more than two materials for segmented branches is used for different ranges of temperature.

Applying the recently-proposed approach [21] for the system shown in Figure 12, the equivalent thermoelectric figure of merit is given by,

$$Z_{eq-series} = \frac{\left(\frac{K_3 \left(\frac{K_2 \alpha_1 + K_1 \alpha_2}{K_1 + K_2} \right) + \frac{K_1 K_2}{K_1 + K_2} \alpha_3}{\frac{K_1 K_2}{K_1 + K_2} + K_3} \right)^2}{\left(R_1 + R_2 + R_3 + \frac{\left(\frac{K_2 \alpha_1 + K_1 \alpha_2}{K_1 + K_2} - \alpha_3 \right)^2}{\frac{K_1 K_2}{K_1 + K_2} + K_3} \frac{(T_{hot} + T_{cold})}{2} + \frac{(\alpha_1 - \alpha_2)^2}{K_1 + K_2} \left(\frac{T_{hot} + T_{i-(1,2)}}{2} \right) \right) \left(\frac{\frac{K_1 K_2 K_3}{K_1 + K_2}}{\frac{K_1 K_2}{K_1 + K_2} + K_3} \right)} \quad (20)$$

where $T_{i-(1,2)}$ is the intermediate temperature between the TEM_1 and TEM_2 . In Equation (20), we have expressed $T_{i-(2,3)}$ in terms of T_{hot} and T_{cold} , but we have no analytical expression for $T_{i-(1,2)}$ temperature. Thus, this case need major revision in future work. However, now, we show the variation of $Z_{eq-series}$ as a function of $T_{i-(1,2)}$ using three different materials, namely $TEM_1 = BiTe$, $TEM_2 = PbTe$ and $TEM_3 = SiGe$. Figure 13 shows the variation of $Z_{eq-series}$ as a function of T_i .

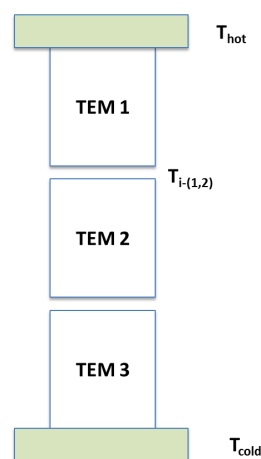


Figure 12. Three-TEM chain thermally and electrically connected in series.

Notice that the values of $T_{i-(1,2)}$ are in the range from 373 K to 1273 K. For this range of temperatures, we have an approximate value of $Z_{eq-series} \approx 0.000595$. If the system were composed of more than three TEMs, as can be inferred, the case is more complex. In this case, we would have a set of unknowns $T_{i-(m,n)}$, (being m, n) each couple of TEMs in the chain. Comparing the value of $Z_{eq-series} \approx 0.000595$ of this three-TEM chain with the values of Z_{eq} corresponding to (SC, PSC, TEP)-CTEGs, we clearly confirm that these systems reach a higher value of Z_{eq} .

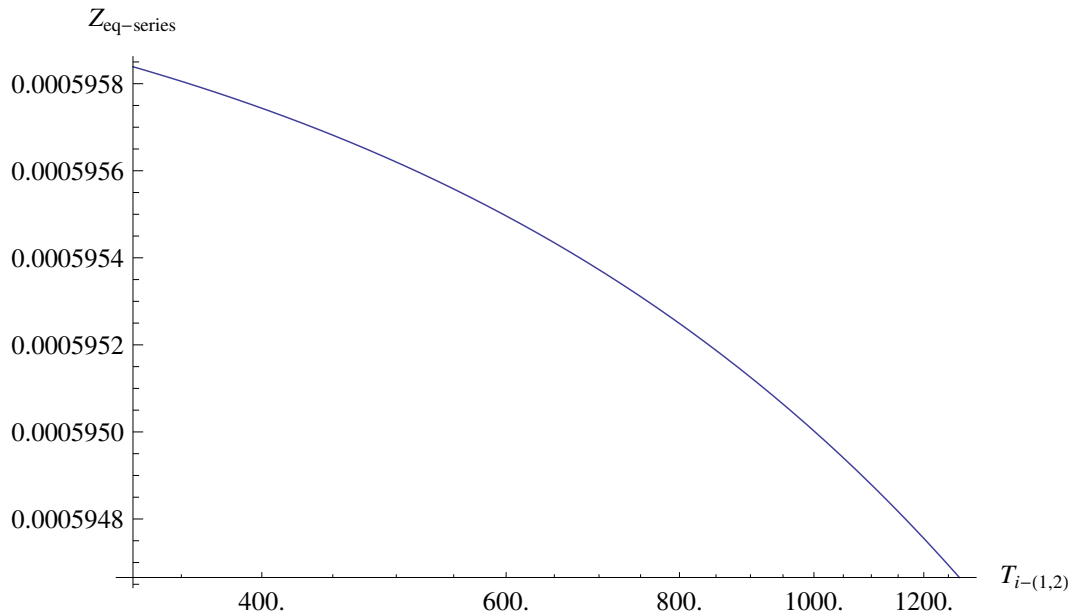


Figure 13. Equivalent figure of merit for the series-system as a function of $T_{i-(1,2)}$, assuming three different materials.

6. Corollary: Maximum Z_{eq} for a CTEG

Our main results can be expressed in the following corollary: In the design of a composite thermoelectric generator CTEG composed of three TEMs, two aspects should be considered:

- (i) There exists a thermal-electrical connection between TEMs, which have the maximum value of Z_{eq} when the thermoelectric material is the same for all TEMs.
- (ii) If different thermoelectric materials are used for each TEM, under the condition $TEM_i = TEM_j \neq TEM_l$ where i, j, l can be 1, 2 or 3, then for a given thermal-electrical connection, there exists an optimal arrangement of the thermoelectric material in which the value of Z_{eq} is maximum.

7. Conclusions

In this work, we have studied the role of the thermoelectric properties on the equivalent thermoelectric figure of merit of a composed thermoelectric system. It has been shown that there are two conditions that affect the performance of a thermoelectric system: (1) the thermal and electrical connection between TEMs; and (2) the arrangement (cyclic order) of thermoelectric materials. In fact, the Z_{eq} of the CTEG composed of three TEMs shows different maximum values using the same thermoelectric material for each TEM, *i.e.*, $TEM_1 = TEM_2 = TEM_3$, but under different configurations, *i.e.*, under different thermal and electrical connections. For example, we found that for the case of the BiTe material, a higher value of Z_{eq} is obtained for the configuration PSC compared to the SC and TEP configurations.

Furthermore, Z_{eq} have different maximum values, when we use two different materials for the TEMs, *i.e.*, under the condition $TEM_i = TEM_j \neq TEM_l$. In this case, we found that the PSC-configuration is the most efficient configuration followed by the TEP and SC configurations, respectively. Furthermore,

we found that the PSC-configuration, using BiTe and PbTe for the TEMs, reaches low values when $TEM_1 = TEM_3 \neq TEM_2$ and $TEM_2 = TEM_3 \neq TEM_1$, but the optimal performance is obtained with the arrangement $TEM_1 = TEM_2 = PbTe \neq TEM_3 = BiTe$.

For completeness, we have shown the effect of contact thermal conductance on the Z_{eq-PSC}^{Inh} for the more efficient case, PSC-CTEG system, in terms of both the ratio $K_3/K_{1,2}$ (intrinsic thermal conductances) and $R_3/R_{1,2}$ (intrinsic electrical resistance).

The arrangements proposed in this work have the advantage that they can achieve a higher figure of merit value compared to a conventional thermoelectric module, in particular the PSC-CTEG system. We have shown that a thermal connection in series of two modules improves the performance when they are thermally connected in parallel with a third TEM, resulting in a higher value of Z .

These results are useful for the design of new thermoelectric systems with the optimal combination of materials to form the legs of the thermocouples in multistage thermoelectric systems, each stage with different material. Thus, our analysis shows elements of validation, which allows one to select: (1) the best thermal and electrical connection; (2) the best materials; and (3) the corresponding position in the arrangement. For future work, we consider it very important to include geometric factors and other extrinsic factors, such as the electrical contact resistance, for more realistic results. Additional later work is required to generalize our results for a system of N modules.

Acknowledgments

This work was financially supported by Instituto Politecnico Nacional (Research Grant 20150488) and CONACYT-Mexico (Research Grant 251141). Alexander Vargas-Almeida was partially financially supported by CONACYT-Mexico (Scholar Grant No. 395825). The authors acknowledge the editorial assistance of the editors to improve the manuscript.

Author Contributions

Alexander Vargas-Almeida and Miguel Angel Olivares-Robles designed the research. Alexander Vargas-Almeida calculated the data. Miguel Angel Olivares-Robles and Alexander Vargas-Almeida analyzed the data. Federico Méndez Lavielle read and commented on the manuscript. Miguel Angel Olivares-Robles and Alexander Vargas-Almeida wrote the paper. All authors have read and approved the final manuscript.

Conflicts of Interest

The authors declare no conflict of interest.

Abbreviations

Symbol	Name
CTEG	Composite thermoelectric generator
Z	Thermoelectric figure of merit
α	Seebeck coefficient
κ	Thermal conductivity
ρ	Electrical resistivity
T_{hot}	Hot side temperature
T_{cold}	Cold side temperature
ΔV	Potential difference
ΔT	Temperature difference
S	Entropy per carrier
e	Electron charge
s	Compatibility factor
SC	Series connection
Z_{eq-SC}	Equivalent figure of merit for the SC system
PSC	Parallel segmented conventional-CTEG
Z_{eq-PSC}	Equivalent figure of merit for the PSC system
TEP	Thermally and electrically in parallel
Z_{eq-TEP}	Equivalent figure of merit for the TEP system
R	Electrical resistance
K	Thermal conductance
Z_{eq-SC}^h	Equivalent figure of merit for the SC system, homogeneous
Z_{eq-PSC}^h	Equivalent figure of merit for the PSC system, homogeneous
Z_{eq-TEP}^h	Equivalent figure of merit for the TEP system, homogeneous
Z_{eq-SC}^{Inh}	Equivalent figure of merit for the SC system, heterogeneous
Z_{eq-PSC}^{Inh}	Equivalent figure of merit for the PSC system, heterogeneous
Z_{eq-TEP}^{Inh}	Equivalent figure of merit for the TEP system, heterogeneous
P_{max}	Maximum power
$P_{max-PSC}$	Maximum power of the PSC system
K_c	Contact thermal conductance
$K_{I=0}$	Thermal conductance at zero electrical current
η	Efficiency of the thermoelectric generator
η_{eq-PSC}^{Inh}	Efficiency of the PSC system, heterogeneous
$Z_{eq-series}$	Equivalent figure of merit for the series system
K_{conv}	Thermal conductance for the heat conveyed by the electrical current
K_{eq}	Thermal conductance of the TEG
I_{eq}	Equivalent electrical current
I_{Qeq}	Equivalent heat flux inside the TEG
α_{eq}	Equivalent Seebeck coefficient
ΔV	Voltage

References

1. Reznikov, M.; Wilkinson, P. Electric Power Generation at Low Temperature Gradients. *IEEE Trans. Ind. Appl.* **2014**, *50*, 4233–4238.
2. Fagas, G.; Gammaitoni, L.; Paul, D.; Berini, G.A. Thermoelectric Energy Harvesting. In *ICT-Energy-Concepts Towards Zero-Power Information and Communication Technology*; InTech: Rijeka, Croatia, 2014.
3. Brief History of Thermoelectrics. Available online: <http://thermoelectrics.caltech.edu/thermoelectrics/history.html> (accessed on 23 October 2015).
4. Snyder, G.J. Small thermoelectric Generators. *Electrochem. Soc. Interface* **2008**, *17*, 54–56.
5. Baetman, P.J. *Some Notes on the Possible Application of Thermoelectric Devices to the Generation of Electric Power*; A.R.C. Technical Report; Her Majesty's Stationery Office: London, UK, 1960.
6. Nolas, G.S.; Sharp, J.; Goldsmid, H.J. *Thermoelectrics*; Springer: Heidelberg/Berlin, Germany, 2001.
7. Callen, H.B. The Application of Onsager's Reciprocal Relations to Thermoelectric, Thermomagnetic, and Galvanomagnetic Effects. *Phys. Rev.* **1948**, *73*, doi:10.1103/PhysRev.73.1349.
8. Nemir, D.; Beck, J. On the Significance of the Thermoelectric Figure of Merit *Z*. *J. Electron. Mater.* **2010**, *39*, 1897–1901.
9. Shakouri, A. Recent Developments in semiconductor thermoelectric physics and materials. *Annu. Rev. Mater. Res.* **2011**, *41*, 399–431.
10. Snyder, G.J.; Toberer, E.S. Complex thermoelectric materials. *Nat. Mater.* **2008**, *7*, 105–114.
11. Hsu, C.T.; Huang, G.-Y.; Chu, H.-S.; Yu, B.; Yao, D.-J. An effective seebeck coefficient obtained by experimental results of a thermoelectric generator module. *Appl. Energy* **2011**, *88*, 5173–5179.
12. Barron, K.C. Experimental Studies of the Thermoelectric Properties of Microstructured and Nanostructured Lead Salts. Master's Thesis, Massachusetts Institute of Technology, Cambridge, MA, USA, 2005.
13. Hurwitz, E.N.; Asghar, M.; Melton, A.; Kucukgok, B.; Su, L.Q.; Oroc, M.; Jamil, M.; Lu, N.; Ferguson, I.T. Thermopower study of GaN-based materials for next-generation thermoelectric devices and applications. *J. Electron. Mater.* **2011**, *40*, 513–517.
14. Thermoelectric Engineering. Available online: <http://thermoelectrics.matsci.northwestern.edu/thermoelectrics/engineering.html> (accessed on 23 October 2015).
15. Snyder, G.J.; Ursell, T.S. Thermoelectric efficiency and compatibility. *Phys. Rev. Lett.* **2003**, *91*, 148301.
16. Safa, K. Thermoelectric Effects in Metals: Thermocouples. Available online: <http://www.kasap.usask.ca/samples/Thermoelectric-Seebeck.pdf> (accessed on 23 October 2015).
17. Apertet, Y.; Ouerdane, H.; Goupil, C.; Lecoq, P. Internal convection in thermoelectric generator models. *J. Phys. Conf. Ser.* **2012**, *395*, 012103.
18. Apertet, Y.; Ouerdane, H.; Goupil, C.; Lecoq, P. Thermoelectric internal current loops inside inhomogeneous systems. *Phys. Rev. B* **2012**, *85*, 033201.

19. Vargas-Almeida, A.; Olivares-Robles, M.A.; Camacho-Medina, P. Thermoelectric System in Different Thermal and Electrical Configurations: Its Impact in the Figure of Merit. *Entropy* **2013**, *15*, 2162–2180.
20. Apertet, Y.; Ouerdane, H.; Glavatskaya, O.; Goupil, C.; Lecoœur, P. Optimal working conditions for thermoelectric generators with realistic thermal coupling. *Europhys. Lett.* **2012**, *97*, doi:10.1209/0295-5075/97/28001.
21. Apertet, Y.; Ouerdane, H.; Goupil, C.; Lecoœur, P. Equivalent parameters for series thermoelectrics. *Energy Convers. Manag.* **2015**, *93*, 160–165.

© 2015 by the authors; licensee MDPI, Basel, Switzerland. This article is an open access article distributed under the terms and conditions of the Creative Commons Attribution license (<http://creativecommons.org/licenses/by/4.0/>).